SUPPLEMENTAL MATERIAL AND METHODS

Plasmid construction

The plasmids pMSCV-neo-*KMT2A-MLLT1*, pGCDNsam-*KMT2A-MLLT1-IRES-Kusabira-Orange*, pMYs-3×*FLAG-Evi1*-IRES-GFP, pMYs-*HoxA9-IRES-Meis1*, and pGCDNsam-*MOZ-TIF2-IRES-EGFP* have been described previously [1-3]. shRNA constructs on the pSIREN-RetroQ-puro and pSIREN-RetroQ-DsRed-Express backgrounds (Clontech Japan, Tokyo, Japan) were generated according to the manufacturer's instructions. For the plasmids used for reporter assays, we amplified genomic DNA from the tail of C57B6 mice with the primers shown in supplemental table 2 with restriction enzyme cleavage sites and cloned them into the firefly luciferase reporter gene plasmid pGL4.10 or pGL4.23 (Promega, Madison, WI). According to the manufacturer's manual, KOD-Plus-Mutagenesis Kit (Toyobo, Japan) was used to delete consensus motifs from the reporter plasmids using the primers shown in supplemental table 2.

Retrovirus production, transduction, and cell selection

Briefly, Plat-E packaging cells were transiently transfected with 6-12 μg of each retrovirus vector mixed with 48-96 μl of polyethylenimines (PEI) and 500 μl of 150 mM

NaCl, followed by incubation at 37℃. The culture medium was replaced 12 hours after transfection. The retrovirus-containing supernatant was collected 24 hours after medium change, filtered through a 0.45 μm filter, and added to the culture plate coated with RetroNectin (Takara Bio, Japan). The culture plate was centrifuged at 2000 × g, 37℃ for 4 hours, and the supernatant was discarded. Cells were seeded onto the virus-coated plate and infected with retroviruses for 24 hours. For puromycin selection, puromycin was added at the concentration of 1 μg/mL at least from 24 to 72 hours after the start of infection, where > 99% of cells without retroviral transduction died. After 48 hours of selection, surviving cells were used for further experiments. Puromycin was continuously added to the culture medium after that.

In vitro culture

Murine AML cells and immortalized cells were maintained in RPMI 1640 supplemented with 10% FCS, 1% PS, 50 ng/mL murine recombinant stem cell factor, 20 ng/mL murine recombinant thrombopoietin, and 20 ng/mL murine recombinant interleukin 3. Palbociclib (Medchemexpress) and Fascaplysin chloride (Cayman) were added to the culture medium, and the medium was changed by half once per day.

Colony-forming assay

An indicated number of cells were seeded in duplicate and cultured in cytokine-supplemented methylcellulose media (MethoCult GF M3434, Stem Cell Technologies, Vancouver, Canada) as per the manufacturer's instructions, and colonies were counted on day 7. The average colony number was adopted as the measurement value.

Transplantation assay

Sublethally irradiated (4.5 - 6.5 Gy) mice were intravenously injected with an indicated number of AML cells, depending on the experiments. Recipient mice were clinically monitored at least once in three days, and a complete blood count was performed once in 1-12 weeks, depending on the model of AML and as indicated. The frequency of AML cells in the peripheral blood was monitored by FACSCelesta (Becton, Dickinson and Company, Japan: BD, Tokyo, Japan) as indicated. The mice were euthanized when they showed clinical signs of illness, including anemia, malaise, and cachexia.

Flow cytometry

A mixture of antibodies for CD3ε (AB_312668 (BioLegend Cat . No. 100303)), CD4 (RRID: AB_312688 (BioLegend Cat. No. 100403)), CD8 (RRID: AB_312742

(BioLegend Cat. No. 100703)), CD127 (RRID: AB_466587 (eBiosience Cat. No. 13-1271-81)), B220 (RRID: AB_312988 (BioLegend Cat. No. 103203)), Gr-1 (RRID: AB_313368 (BioLegend Cat. No. 108403)), Mac-1 (RRID: AB_466359 (eBiosience Cat. No. 13-0112-82)), and Ter-119 (RRID: AB_313704 (BioLegend Cat. No. 116203)) was used to identify lineage$^+$ cells. Dead cells were excluded using DAPI (4',6-diamidino-2-phenylin-dole) (BD) or 7-AAD (7-amino-actinomycin D) (BD) according to the manufacturer's instructions. We defined L-GMPs as follows; GFP$^+$ (when applicable), lineage (Gr-1, B220, CD3, CD4, CD8, CD127, Ter119)-negative, c-kit+, Sca-1-, CD16/32+ and CD34+. The data were analyzed with FlowJo software (Tree Star, Ashland, OR, USA, RRID:SCR_008520)).

Cell cycle analysis

One million EVI1-AML cells undergoing 72-hour puromycin selection following transduction of shRNA cloned into pSIREN-RetroQ-puro were fixed in ice-cold 70% ethanol overnight. Cells were incubated with 1 μg/mL DAPI and 0.1% Triton X-100 for 30 minutes at room temperature before analysis using FACSCelesta. Mean + SD from 3 independent experiments were shown.

Apoptosis assay

One million EVI1-AML cells 48 hours after transduction of shRNA cloned into pSIREN-RetroQ-DsRed were stained with Annexin V-APC (BD, RRID:AB_2868885) and DAPI (1 μg/ml) according to manufacturer's instructions. The frequency of annexin V^+ $DAPI^-$ cells and $DAPI^+$ cells were analyzed with FACSCelesta gating on $DsRed^+$ cells. Data were shown as mean + SD from 3 independent experiments.

Magnetic cell separation of spleen T and NK cells

To obtain spleen T cells, $CD3^+$ T cells were separated using CD3ε biotin-conjugated antibody, Streptavidin MicroBeads, and autoMACS (Miltenyi Biotec, Bergisch Gladbach, Germany) according to the manufacturer's protocol. Residual cells underwent further separation of $CD49b^+$ NK cells using the same protocol. Cells were used for RNA isolation after > 90% purity was confirmed using FACSCelesta.

Real-time quantitative PCR (qPCR)

Total RNA was prepared using Nucleospin-RNA II or RNA XS kit (Macherey-Nagel, Düren, Germany) and reverse-transcribed into cDNA with ReverTra Ace qPCR RT Master Mix (Toyobo, Osaka, Japan). Real-time qPCR was carried out on the

LightCycler480 (Roche) or QuantStudio system (Thermo Fisher) using SYBR green reagents in triplicate. Relative expression was normalized to the internal control. The list of primers used in qPCR is provided in Supplemental Table 2.

Western blot

Primary antibodies used are as follows: anti-ERG (CST cat# 97249, RRID:AB_2721841), anti-Cyclin D1 (CST cat#55506, RRID:AB_2827374), anti-STAT1 (BD cat# 610185, RRID:AB_397584), anti-β-Actin (CST cat#4967, RRID:AB_330288). Secondary antibodies used are anti-rabbit IgG, HRP-linked antibody (CST cat#7074, RRID:AB_2099233) and anti-mouse IgG, HRP-linked antibody (CST cat#7076, RRID:AB_330924). Western blotting was performed according to the protocol provided by CST.

Luciferase reporter assay

For analysis of luciferase activities, COS-7 cells were seeded in 96-well culture plates at a density of 1×10^5 per well. The cells were transfected with 100 ng of pGL4.23, pGL4.10, or an equimolar amount of each reporter construct, together with 100 ng of pME18S or an equimolar amount of pME18S-EVI1 expression plasmid and 2 ng of pRL-TK with

PEI. After 48 hours of culture, cells were harvested, and luciferase activities were measured in an ARVO MX (PerkinElmer, Waltham, MA) with a Dual-Glo luciferase assay system E2920 (Promega) to derive firefly and Renilla relative light unit values (RLU) from the same cell extract. To calculate the fold-change in reporter expression due to EVI1 expression, the firefly luciferase RLU was divided by the Renilla luciferase RLU value to give a normalized value, and then the normalized value was divided by the normalized value from the empty pGL4-Luc to give the fold-change. Data are expressed as mean + SD from 3 or more separate experiments.

ChIP-sequencing analysis

ChIP experiments were carried out using 2×10^6 cells. The antibodies used in ChIP assays were Monoclonal Anti-FLAG M2 (F3165, Sigma-Aldrich, Cat# F3165, RRID:AB_259529), anti-histone H3 (tri methyl K4) antibody (cat# ab8580, RRID:AB_306649) and normal mouse IgG (Santa Cruz Biotechnology, Cat# sc-2025, RRID:AB_737182). Bound DNA fragments were eluted and quantified by subsequent qPCR. The data were analyzed as previously described [4]. Briefly, reads were aligned to the mouse genome build mm10 using Bowtie2 version 2.4.1 [5] with default parameters. Quality assessment, read normalization, peak calling, and visualization were performed

by SSP version 1.2.2 [6] and DROMPAplus version 1.12.1 [7]. The default parameter set was used for peak calling ("100-bp bin, --pthre_internal=5, --pthre_enrich=4").

ChIP-qPCR analysis

ChIP experiment using anti-FLAG antibody was performed as described above. ChIP against EVI1 (CST cat# 2593, RRID:AB_2184098) in human HNT-34 AML cell line was performed employing first cross-linking for 45 minutes with DSG (disuccinimidyl glutarate, ThermoFisher cat#20593) before formaldehyde cross-linking. qPCR was carried out on the QuantStudio system (Thermo Fisher) using SYBR green reagents in triplicate. The relative amount was normalized to the input genome DNA. The list of primers used in ChIP-qPCR is provided in Supplemental Table 2.

RNA-sequencing (RNA-seq) analysis

The quality of the RNA samples (RNA Integrity Number > 9.5) was validated using an Agilent 2100 Bioanalyzer (Agilent Technology). Total RNA was submitted to the Genewiz sequencing facility (Jiangsu, China), then enrichment Poly-A RNAs for library preparation and strand-specific total RNA sequencing on the NovaSeq platform. FastQC (RRID:SCR_014583) was used to perform RNA-seq data quality control with the default

parameters. Sequencing reads were mapped to GRCm39 by HISAT2 (v2.2.1, RRID:SCR_015530) using default parameters. For pathway analysis, GSEA software (RRID:SCR_005724) on the Java platform (v4.1.0) was used [8,9].

Single-cell RNA-sequencing (scRNA-seq) datasets

By using the Seurat R package, cells with a unique feature count over 3000, less than 200, and ≥ 10% mitochondrial counts were filtered, followed by normalization using Seurat "NormalizeData" function with a scale factor of 10,000 and scaling using "ScaleData" function. The "Elbowplot" function was used to select dimensionality. Non-linear dimension reduction was performed by the "RunUMAP" function. Cells annotated as AML cells by the authors were used to draw a diagram [10]. Violin plot and two-color dot plot were drawn using "VlnPlot" and "FeaturePlot" functions.

Data from two patients were used as $EVI1^{+}$-AML. AML328 is characterized by DNMT3A c.1910T>A p.L637Q, TP53 c.431A>C p.Q144P, c.455C>G p.P152R and FLT3-ITD with karyotype 45, XX, ider(3)(q10), inv(3)(q21q26.2), add(5)(q13), -7, add(9)?dup(q13q22). AML870 is characterized by ZRSR2 c.1147C>G p.P383A with karyotype 46, XY, t(9;11)(p21;q23).

Data analysis using publicly available genetic data

For selecting genes positively correlated to *EVI1* using the transcriptome data [11], the expressions of *EVI1* (215851_at and 221884_at) were used as a phenotype on the GSEA software (v4.1.0) [8,9], and genes with a score of more than 0.15 in both lists were selected.

For anti-ERG ChIP-seq, all available anti-ERG ChIP-Seq profiles of AML cells except acute promyelocytic leukemia were integrated from the ChIP-Atlas resource (http://chip-atlas.org, RRID:SCR_015511) [12]. AML data (GSM2026052, GSM1122314, and GSM585590) were compared to that of normal $CD34^+$ progenitor cells (GSM585604) [12-15]. The binding of ERG to each gene locus given by Peak Browser on ChIP-Atlas was normalized to Z score. Genes for which the average Z-score in AML cells was at least 1 greater than in normal $CD34^+$ cells were submitted to gene ontology (GO) analysis.

For GO analysis of positively correlated genes with *ERG*, genes that were positively correlated with ERG in OHSU datasets with a q-value less than 0.01 were submitted to GO analysis.

SUPPLEMENTAL FIGURE LEGENDS

Supplemental figure 1. *Evi1*^{high} cells show distinct features in murine AML models.

A. UMAP plot of sc-RNA-seq data of AML cells from patient AML870 with t(9;11)(p21;q23), showing 4 clusters. **B.** Violin plot of MECOM expression in the 4 clusters. **C.** Representative flow-cytometric data showing GFP (EVI1) positivity within the whole live leukemia cells and L-GMPs. **D.** Flow cytometric evaluation of KuO of GFP^{high} and GFP^{low} L-GMPs from KMT2A-MLLT1 AML harboring the *Evi1*-KI allele. **E.** Representative flow cytometric data of the bone marrow of secondary recipient mice transplanted with GFP^{high} and GFP^{low} L-GMPs as indicated. Both GFP^{high} and GFP^{low} fractions were generated from both GFP^{high} and GFP^{low} cells. **F-H.** A Kaplan-Meier survival curve for secondary recipient mice transplanted with an indicated number of GFP^{high} or GFP^{low} L-GMPs, after exposure to 6.5 Gy TBI. Significance between the same number of cells was examined by a log-rank test. **I-J.** GSEA showing that differentiation-related genes in HSCs (**I**) and doxorubicin-resistance-related genes (**J**) are up-regulated in GFP^{high} L-GMPs. **K.** A model of the experiment to analyze the effect of exogenous expression of *Evi1* in KMT2A-MLLT1 AML cells. pMYs-IRES-GFP or pMYs-*Evi1*-IRES-GFP retroviral constructs were used to transduce freshly isolated KMT2A-MLLT1 AML cells. After 48-hour culture, 20,000 GFP^{+} cells were transplanted into primary

recipient mice. After AML development, 200 GFP^+ cells were subjected to colony-forming and transplantation assay into secondary recipient mice. **L.** A Kaplan-Meier survival curve for primary recipient mice.

FDR: false discovery rate (q-value), GSEA: gene set enrichment analysis, HSC: hematopoietic stem cells, KuO: Kusabira-Orange, L-GMP: leukemic granulocyte-macrophage progenitor, NES: normalized enrichment score, UMAP: Uniform Manifold Approximation and Projection.

Mean ± S.D. * $p < 0.05$.

Supplemental figure 2. A combination of multimodal screening showed potential targets of EVI1 in AML cells.

A. Expression of *Evi1* mRNA in EVI1-AML, compared to normal LSKs. **B.** ChIP-qPCR analysis using anti-FLAG antibody showing the binding of 3×FLAG-tagged EVI1 to the known EVI1-binding regions in the EVI1-AML samples. *Gata2* and *Pten* are positive controls, and *Alb* is a negative control. **C.** Distribution of binding sites of EVI1, elucidated by ChIP-seq using anti-FLAG antibody in the EVI1-AML samples. **D.** ChIP-qPCR analysis using anti-FLAG antibody showing the binding of 3×FLAG-tagged EVI1 to the EVI1-binding regions identified in the ChIP-seq of the EVI1-AML samples. Neighborhood sequences without enrichment in the ChIP-seq were used as a negative control.

Alb: Albumin, ChIP: chromatin immunoprecipitation, *Gata2*: GATA binding protein 2, *Pten*: Phosphatase and tensin homolog, qPCR: quantitative PCR.

Mean ± S.D. ** $p < 0.01$.

Supplemental figure 3. ERG and CCND1 are targets of EVI1 in *Evi1*^{high} AML cells.

A. Detailed illustration of the results of ChIP-seq in the murine *Erg* locus, aligned with the public ChIP-seq data of major hematopoietic transcription factors in an HPC-7 murine hematopoietic progenitor cell line[16]. Blue bars represent the regi ons cloned into the pGL4.23-luciferase reporter construct. **B-C.** Relative luciferase activity of *Erg* reporter constructs in COS-7 cell lysates transiently transfected with EVI1 compared with that without EVI1. Data were normalized to those of empty pGL4.23 plasmid and shown as mean + SD from 4 independent experiments. **D.** Detailed illustration of the results of ChIP-seq in the murine *Ccnd1* locus, aligned with the public ChIP-seq data of major hematopoietic transcription factors in an HPC-7 murine hematopoietic progenitor cell line[16]. Blue bars represent the regions cloned into the reporter construct. **E-F.** Relative luciferase activity of *Ccnd1* reporter constructs in COS-7 cell lysates transiently transfected with EVI1 compared with that without EVI1. Data were normalized to those of empty pGL4.23 plasmid and shown as mean + SD from 4 independent experiments. **G-H.** The regions corresponding to the murine *Erg* +85 and *Ccnd1* -4.0 - -3.6, which EVI1 binds to in murine AML cells and show activating capacity in reporter assays (indicated in the black bar). The amplicons used in anti-EVI1 ChIP-qPCR were shown as ChIP qPCR 1 and 2. Dnase I hypersensitivity sites and transcription factor binding sites

241 in various cell lines, EVI1-binding consensus motifs (familial profile 241 and 95439380),
242 the conserved area in the vertebrae, and Dnase I hypersensitivity sites in the human
243 primary AML cells with inv(3) are shown [17,18]. **I-J.** GSEA shows that EWS-ETS and ERG
244 fusion protein target genes in solid cancers are up-regulated in GFP^{high} L-GMPs. **K.**
245 Colony-forming activity of 500 c-kit^{+} normal hematopoietic progenitor cells transduced
246 with shRNAs against indicated genes.
247 FDR: false discovery rate (q-value), GSEA: gene set enrichment analysis, L-GMP:
248 leukemic granulocyte-macrophage progenitor, NES: normalized enrichment score.
249 Mean ± S.D. * $p < 0.05$, ** $p < 0.01$.
250

Supplemental figure 4. *Evi1*^{high} AML cells are dependent on ERG.

A. Quantitative PCR showing the relative expression of *Erg* in EVI1-AML cells expressing sh*Erg* in vitro. **B.** Western blotting showing the efficacy of *Erg* silencing in EVI1-AML cells. **C.** Cell cycle analysis of EVI1-AML cells transduced with shRNAs against *Luciferase* and *Erg.* The sub-G1 peak represents hypodiploid apoptotic cells. **D.** Apoptosis analysis of EVI1-AML cells transduced by shRNAs against *Luciferase* and *Erg* with DsRed**.** Frequency of annexin V^+ $DAPI^-$ early apoptotic cells (Annexin V+) and DAPI+ dead cells (DAPI+) in DsRed-labeled $EVI1^+$ AML cells were shown. **E.** A model of bone marrow transplantation experiments. **F.** A model of establishment of KMT2A-MLLT1-transduced immortalized cell clones. **G.** Expression of GFP-EVI1 in different KMT2A-MLLT1 clones. **H.** Expression of *Evi1* mRNA in different KMT2A-MLLT1 clones, compared to normal LSKs. **I.** Relative cell proliferation of KMT2A-MLLT1 CL1 cells expressing shRNAs against *Luciferase* and *Erg* in vitro. **J.** Colony-forming units of KMT2A-MLLT1 CL1 cells expressing shRNAs against *Luciferase* and *Erg.* **K.** A Kaplan-Meier survival curve for recipient mice transplanted with 1×10^6 HOXA9-MEIS1 AML cells expressing shRNAs against *Luciferase* and *Erg* after being exposed to 6.5 Gy TBI. **L.** A 2D dot plot showing the relationship between differentially expressed genes after *Erg* deletion in normal HSCs and *Erg* knockdown in EVI1-AML cells. **M.** A volcano plot

showing differentially expressed genes in EVI1-AML cells with *Erg* silencing. **N.** GSEA showing that MYC-target genes are down-regulated in EVI1-AML cells with *Erg* silencing. **O.** Top listed GO biological processes of differentially binding regions in publicly available ChIP-seq data using an anti-ERG antibody between normal $CD34^+$ cells and AML cell lines (Kasumi-1 (GSM2026052), ME-1 (GSM1122314) and SKNO-1 (GSM585590)). **P.** Top listed GO biological processes positively correlated with *ERG* with a q-value < 0.01 in the OHSU datasets.

ChIP: chromatin immunoprecipitation, CL: clone, FDR: false discovery rate (q-value), , GO: gene ontology, GSEA: gene set enrichment analysis, NES: normalized enrichment score, OHSU: Oregon Health Sciences University.

Mean ± S.D. * $p < 0.05$, ** $p < 0.01$, *** $p < 0.001$.

Supplemental figure 5. Cyclin D1 is necessary for the efficient development of EVI1-AML in vivo.

A. Quantitative PCR showing the relative expression of *Ccnd1* in EVI1-AML cells expressing sh*Ccnd1* in vitro. **B.** Western blotting showing the efficacy of *Ccnd1* silencing in EVI1-AML cells. **C.** Cell cycle analysis of EVI1-AML cells transduced with shRNAs against *Luciferase* and *Ccnd1*. **D.** Relative cell proliferation of KMT2A-MLLT1 CL1 cells expressing shRNAs against *Luciferase* and *Ccnd1* in vitro. The data for sh*Luciferase* are common to those of supplemental figure 4I. **E.** Colony-forming units of KMT2A-MLLT1 CL1 cells expressing shRNAs against *Luciferase* and *Ccnd1*. The data for sh*Luciferase* are common to those of supplemental figure 4J. **F.** Relative cell proliferation of AML cells with sh*Ccnd1* compared to those with sh*Luciferase*, through days 0 to 3. A comparison was made within the same cell between sh*Luciferase* and sh*Ccnd1*.**G.** Relative cell proliferation of different clones of KMT2A-MLLT1 transformed cells (Supplemental figure 4F) with indicated concentrations of palbociclib compared to that with vehicle (0 μM), through days 0 to 3. Clones were characterized by different expression levels of GFP (*Evi1*). A relative cell number was compared to EVI1^{low} CL1 cells at the same concentration. **H-I.** Relative cell proliferation of murine AML cells with indicated concentrations of palbociclib (H) and fascaplysin (I) compared to that with

vehicle (0 μM), through days 0 to 3. A relative cell number was compared to EVI1-AML cells at the same concentration. **J.** Frequency of GFP^+ cells in the bone marrow of lethally irradiated (8.5 Gy) recipient mice infused with 5×10^6 AML cells, 16 hours after transplantation.

CL: clone.

Mean ± S.D. * $p < 0.05$, ** $p < 0.01$, *** $p < 0.001$.

Supplemental figure 6. Cyclin D1 is associated with IFN signatures and immune exhaustion in EVI1-AML.

A. GSEA showing gene sets associated with positive regulation of cell cycle are not significantly affected by silencing of *Ccnd1*in vitro. **B.** GSEA showing gene sets associated with response to interferon-γ are down-regulated by silencing of *Ccnd1* in vitro. **C.** GSEA showing gene sets associated with the response to type I interferon are down-regulated by silencing of *Ccnd1* in vitro. **D.** GSEA showing gene sets associated with the chemokine signaling are down-regulated by silencing of *Ccnd1* in vivo. **E.** Detailed illustration of the results of ChIP-seq in the murine *Stat1* promoter region. A blue bar represents the regions cloned into the pGL4.10-luciferase reporter construct. **F.** Relative luciferase activity of *Stat1* promoter constructs in COS-7 cell lysates transiently transfected with EVI1 compared with that without EVI1. Data were normalized to those of empty pGL4.10 plasmid and shown as mean + SD from 3 independent experiments. **G.** Quantitative PCR showing the relative expression of *Stat1* in EVI1-AML cells expressing shRNA against *Evi1*. The efficiency of *Evi1* silencing was shown in the Figure 3D. **H.** A model of the experiment to analyze the expression of exhaustion-associated genes in spleen T cells in the early stage of AML development. EVI1-AML cells expressing shRNA from secondary recipient mice were transplanted into tertial recipient

mice without in vitro culture. **I.** A model of the experiment to analyze the composition of T cells infiltrating the liver in the AML mice. **J-K.** Pearson correlation analysis between IFN-γ score and *MECOM / CCND1* expression in OHSU samples. **L.** Pearson correlation analysis between *STAT1* and *MECOM* expression in TCGA samples. **M.** Pearson correlation analysis between *CD274* and *MECOM* expression in TCGA samples. **N.** Pearson correlation analysis between *CD274* and *CCND1* expression in OHSU samples. FDR: false discovery rate (q-value), GSEA: Gene Set Enrichment Analysis, NES: normalized enrichment score, OHSU: Oregon Health Sciences University, TBI: total body irradiation, TCGA: The Cancer Genome Atlas.

Mean ± S.D. * $p < 0.05$, ** $p < 0.01$.

Supplemental figure 7. Overexpression of *CCND1* is associated with type II IFN signature in human AML.

A. Western blotting showing the efficacy of *Stat1* silencing in EVI1-AML cells. **B.** Relative cell proliferation of EVI1-AML cells expressing shRNAs against *Luciferase* and *Stat1* in vitro. **C.** Quantitative PCR showing the relative expression of *Ifngr1* in EVI1-AML cells expressing sh*Ifngr* in vitro. **D.** Quantitative PCR showing the relative expression of *Ifnar1* in EVI1-AML cells expressing sh*Ifnar* in vitro. **E.** A Kaplan-Meier survival curve for recipient mice transplanted with 1×10^6 EVI1-AML cells expressing shRNAs against *Ifnar*, after exposure to 4.5 Gy TBI. **F.** Quantitative PCR showing the relative expression of chemokines and *Stat1* in EVI1-AML cells after treatment of Palbociclib (0.3 μM) for 72 hours. **G.** Pearson correlation analysis between *CCL2* and *CCND1* expression in OHSU samples. **H.** Pearson correlation analysis between *CCL4* and *MECOM* expression in TCGA samples. **I.** Pearson correlation analysis between *CCL4* and *CCND1* expression in OHSU samples. **J.** Pearson correlation analysis between estimated expression *of TIGIT* in CD4 T cells calculated using CIBERSORTx and *MECOM* expression in TCGA samples. **K.** Pearson correlation analysis between estimated expression *of TIGIT* in CD8 T cells calculated using CIBERSORTx and *CCND1* expression in OHSU samples. **L.** Pearson correlation analysis between estimated

expression *of IFNG* in CD8 T cells calculated using CIBERSORTx and *CCND1* expression in OHSU samples. **M.** Pearson correlation analysis between estimated expression *of ICOS* in CD8 T cells calculated using CIBERSORTx and *MECOM* expression in TCGA samples. **N.** Pearson correlation analysis between estimated expression *of LAG3* in NK cells calculated using CIBERSORTx and *MECOM* expression in TCGA samples.

OHSU: Oregon Health Sciences University, TBI: total body irradiation, TCGA: The Cancer Genome Atlas.

Mean ± S.D.

Supplemental table 1. Details of antibodies used for flow cytometry

Epitope	Conjugate	Clone	Concentration	Company
B220	Biotin	RA3-6B2	1:200	BioLegend
CD3e	Biotin	145-2C11	1:200	BioLegend
	PerCP-Cy5.5	145-2C11	1:200	BD
CD4	Biotin	GK1.5	1:200	BioLegend
	PE	GK1.5	1:200	BioLegend
CD8	Biotin	53-6.7	1:200	BioLegend
	PerCP	53-6.7	1:200	BioLegend
CD11b	Biotin	M1/70	1:200	eBioscience
CD16/32	APC	93	1:200	eBioscience
	PE	93	1:200	BioLegend
CD34	FITC	RAM34	1:50	eBioscience
	Alexa Flour 647	RAM34	1:50	BD
CD122	APC	5H4	1:200	BioLegend
CD127	Biotin	A7R34	1:200	eBioscience
	PE	A7R34	1:200	eBioscience
CD279	APC-Cy7	29F.1A12	1:200	BioLegend
c-kit	APC	2B8	1:200	BioLegend
	PE-Cy7	2B8	1:200	BD
Gr-1	Biotin	RB6-8C5	1:200	BioLegend
Sca-1	PE-Cy7	E13-161.7	1:200	BioLegend
	PerCP-Cy5.5	D7	1:200	BioLegend
Streptoavidin	APC-Cy7		1:200	BioLegend
	PerCP-Cy5.5		1:200	BD
Ter-119	Biotin	Ter-119	1:200	BioLegend
TIGIT	PE-Cy7	1G9	1:200	BioLegend

Supplemental table 2. Primers, oligos, and cloning templates used in this study.

Primer	Application	Sequences
sh*Luciferase* F	Construct	TCGAAGTATTCCGCGTACG
sh*Luciferase* R	Construct	CGTACGCGGAATACTTCGA
sh*Erg*-1 F	Construct	AAGTATTACTACAGAAATAGA
sh*Erg*-1 R	Construct	TCTATTTCTGTAGTAATACTT
sh*Erg*-2 F	Construct	GGGAAACTACCTGTGTTTAAAAA
sh*Erg*-2 R	Construct	TTTTTAAACACAGGTAGTTTCCC
sh*Ccnd1*-1 F	Construct	TTGATTCTTTTATATGTTTTT
sh*Ccnd1*-1 R	Construct	AAAAACATATAAAAGAATCAA
sh*Ccnd1*-2 F	Construct	ATGAAATAGTGACATAATATATT
sh*Ccnd1*-2 R	Construct	AATATATTATGTCACTATTTCAT
sh*EVI1* F	Construct	ATCTAAGGCTGAACTAGCAGA
sh*EVI1* R	Construct	TCTGCTAGTTCAGCCTTAGAT
sh*Evi1*-1 F	Construct	ATCTAAGGCTGAACTAGCAGA
sh*Evi1*-1 R	Construct	TCTGCTAGTTCAGCCTTAGAT
sh*Evi1*-2 F	Construct	TCAGTGTCCCAAGGCATTTAA
sh*Evi1*-2 R	Construct	TTAAATGCCTTGGGACACTGA
sh*Evi1*-3 F	Construct	ACAGCAGTGTGAAGCCCTTTA
sh*Evi1*-3 R	Construct	TAAAGGGCTTCACACTGCTGT
shStat*1*-3 R	Construct	TTTAAAGTTATCTCACCAGGC
sh*Ifna*-2 F	Construct	TTTCACAGACACATGTAAATA
sh*Ifna*-2 R	Construct	TATTTACATGTGTCTGTGAAA
sh*Ifng*-1 F	Construct	ACCGACGAATGTTCTAATTAA
sh*Ifng*-1 R	Construct	TTAATTAGAACATTCGTCGGT
sh*Ifng*-2 F	Construct	GATGACAGAAAGGATTCAATT
sh*Ifng*-2 R	Construct	AATTGAATCCTTTCTGTCATC
sh*Dnm3* F	Construct	CTGTGATATAAGCATTCTAAA
sh*Dnm3* R	Construct	TTTAGAATGCTTATATCACAG
sh*Selp* F	Construct	TCCGAAAGATCAACAATAAGT
sh*Selp* R	Construct	ACTTATTGTTGATCTTTCGGA
sh*Etv1* F	Construct	TTGTTTATGAACTGTTAAAGA
sh*Etv1* R	Construct	TCTTTAACAGTTCATAAACAA
sh*Egln3* F	Construct	TTCTTATTCGCACTTTATGTA
sh*Egln3* R	Construct	TACATAAAGTGCGAATAAGAA

sh*Phactr1* F	Construct	TTGACAATTTGACATTAATTA
sh*Phactr1* R	Construct	TAATTAATGTCAAATTGTCAA
sh*Angpt1* F	Construct	AGCTAACAAATGGCTAGTTTT
sh*Angpt1* R	Construct	AAAACTAGCCATTTGTTAGCT
sh*Mkl2* F	Construct	AGGAAAATAAATATTTTTACT
sh*Mkl2* R	Construct	AGTAAAAATATTTATTTTCCT
sh*Hlcs* F	Construct	AAGATACATATATAAAATTTA
sh*Hlcs* R	Construct	TAAATTTTATATATGTATCTT
sh*Ptk7* F	Construct	GAGCTTTTGACACTTATATGA
sh*Ptk7* R	Construct	TCATATAAGTGTCAAAAGCTC
sh*Egfl7* F	Construct	CTCCATCTTTGTCATAATAAA
sh*Egfl7* R	Construct	TTTATTATGACAAAGATGGAG
sh*Nbeal2* F	Construct	GCCAACTATGTCAAAGTTTGA
sh*Nbeal2* R	Construct	TCAAACTTTGACATAGTTGGC
sh*Ogt* F	Construct	ATGAAGAAATTGGTTAGTATT
sh*Ogt* R	Construct	AATACTAACCAATTTCTTCAT
Erg+60 F	Construct	CACAAGTGTGGCCAAGGGCCTCTG
Erg+60 R	Construct	CTGTCAGCTTCCCGGTTTCCCATTCATC
Erg+75 F	Construct	GGCAGAGAGATGATGTCTCAGAAGAGTTGGC
Erg+75 R	Construct	CTGGGCACGGAGAACAACCCGTG
Erg+85 F	Construct	GGTAGGTACCCCGTATCCATTTGTAGCC
Erg+85 R	Construct	GGGCTGCCGTCAACTAAGGTTCCTG
Erg+85 ΔFP241 F	Construct	AATTCAAATCTGGTTGTTTAGTCTACATGGAG CAGGG
Erg+85 ΔFP241 R	Construct	ACGGCCCCTTCACAGATGTGCACAGATG
Erg+85 Δ95439380 F	Construct	ATCTCATTTCCGACAAGACTTCCCTTTCCTTC
Erg+85 Δ95439380 R	Construct	AACGAGTGTTCAGCCCTGATAACCCATCTG
Ccnd1 -0.6 - 0 F	Construct	GACAGGGACGCTGGGATTTCTAAGC
Ccnd1 -0.6 - 0 R	Construct	CTTCGCAGCACAGGAGCTGGTGTTC
Ccnd1 -1.4 - -0.3 F	Construct	CTGGGACACGAAAGTATTCCGTGGGAA
Ccnd1 -1.4 - -0.3 R	Construct	TCGTAGATATGCAAATCGCTCGGACTGC
Ccnd1 -2.4 - -0.3 F	Construct	GGGTTCGAGGAGGCAGGAAATCCG
Ccnd1 -2.4 - -0.3 R	Construct	TCGTAGATATGCAAATCGCTCGGACTGC
Ccnd1 -4.0 - -0.3 F	Construct	TAGTTCCTCTCTGGCTTCTACCACAGTCAG
Ccnd1 -4.0 - -0.3 R	Construct	TCGTAGATATGCAAATCGCTCGGACTGC

Ccnd1 -4.0 - -3.6 F	Construct	TAGTTCCTCTCTGGCTTCTACCACAGTCAG
Ccnd1 -4.0 - -3.6 R	Construct	GGCGGACCCATGGCACTAGCCTC
Ccnd1 -3.8 - -3.6 F	Construct	GTTCACCGCGGGGAGCGTCCTCA
Ccnd1 -4.0 - -3.6 R	Construct	GGCGGACCCATGGCACTAGCCTC
Ccnd1 -4.0 - -3.6 ΔFP241 F	Construct	TAGTTCCTCTCTGGCTTCTACCACAGTCAG
Ccnd1 -4.0 - -3.6 ΔFP241 R	Construct	GTGGCTTGGACGCGCGGGCGGA
Ccnd1 -3.8 - -3.6 ΔFP241 F	Construct	GTTCACCGCGGGGAGCGTCCTCA
Ccnd1 -3.8 - -3.6 ΔFP241 R	Construct	GTGGCTTGGACGCGCGGGCGGA
Stat1 promoter F	Construct	AGTGATGCGCCTACTTAATGCAGGATCTCC
Stat1 promoter R	Construct	GACTCGGCGCTGAAAACCGAAAGTACC
Gapdh F	qPCR	TGGCCTCCAAGGAGTAAGAA
Gapdh R	qPCR	GGTCTGGGATGGAAATTGTG
18s RNA F	qPCR	CGCGGTTCTATTTTGTTGGT
18s RNA R	qPCR	AGTCGGCATCGTTTATGGTC
Erg F	qPCR	AAGGCCATGATCCAGACTGT
Erg R	qPCR	ACTGGTCCTCGCTCACAACT
Ccnd1 F	qPCR	GAGATTGTGCCATCCATGC
Ccnd1 R	qPCR	CTCCTCTTCGCACTTCTGCT
Evi1 F	qPCR	GGAGGAGGACTTGCAACAAA
Evi1 R	qPCR	GACAGCATGTGCTTCTCCAA
Stat1 F	qPCR	GGAGGTGAACCTGACTTCCA
Stat1 R	qPCR	CAAAGGCGTGGTCTTTGTCA
Ifngr F	qPCR	GAGCTTTGACGAGCACTGAG
Ifngr R	qPCR	CCAGGAACCCGAATACACCT
Ifnar F	qPCR	ATCTCCAAGTGGATGCCCAA
Ifnar R	qPCR	TGAATAGCCAGGAAGCCACT
Lag3 F	qPCR	CTCCATCACGTACAACCTCAAGG
Lag3 R	qPCR	GGAGTCCACTTGGCAATGAGCA
Pdcd1 F	qPCR	CCCTAGTGGGTATCCCTGTATT
Pdcd1R	qPCR	TCCTTCAGAGTGTCGTCCTT
Tigit F	qPCR	GCTGACCCACAGGAATACTTTA
Tigit R	qPCR	GAGAGACATAGGGAGAGGGATAG
Ccl2 F	qPCR	GAAGGAATGGGTCCAGACATAC
Ccl2 R	qPCR	TCACACTGGTCACTCCTACA
Ccl4 F	qPCR	CCACTTCCTGCTGTTTCTCTTAC

Ccl4 R	qPCR	GGAGACACGCGTCCTATAACTA
Ccl5 F	qPCR	GCCCACGTCAAGGAGTATTT
Ccl5 R	qPCR	CTGATTTCTTGGGTTTGCTGTG
ChIP PC *Pten* promoter 3 F	ChIP-qPCR	TTTAATTTCCGAGTTTGCGTTAAT
ChIP PC *Pten* promoter 3 R	ChIP-qPCR	AGTAAACTGCCTTGAAGCAAGTGA
ChIP PC *Gata2* promoter 2 F	ChIP-qPCR	CAGGCTCTGGCTGCACCT
ChIP PC *Gata2* promoter 2 R	ChIP-qPCR	TTCCATACCCTACGCTCTCC
ChIP NC *Alb* promoter F	ChIP-qPCR	CTCCAGATGGCAAACATACG
ChIP NC *Alb* promoter R	ChIP-qPCR	TCTGTGTGCAGAAAGACTCG
ChIP *Erg*+85 1 F	ChIP-qPCR	AGAGTGACCCACCCTCCTTT
ChIP *Erg*+85 1 F	ChIP-qPCR	AACGGTTGGACAGAACTTGC
ChIP *Erg*+85 2 F	ChIP-qPCR	CAGGGAGCTGCTTAAACTGG
ChIP *Erg*+85 2 F	ChIP-qPCR	ACTCTTTCCCCGAACTTGGT
ChIP NC *Erg* F	ChIP-qPCR	CTTGAGCTCCACCCTGAGAG
ChIP NC *Erg* R	ChIP-qPCR	TGAATCATGAGGCTCAGCAC
ChIP *Ccnd1* 1 F	ChIP-qPCR	CAGCGGAGCCAAGACAGTAT
ChIP *Ccnd1* 1 R	ChIP-qPCR	CGCTTACCGTAAACCTTGGA
ChIP *Ccnd1* 2 F	ChIP-qPCR	GTCGCGTCCAAGGTTTACG
ChIP *Ccnd1* 2 R	ChIP-qPCR	CTGCTCCCTGTGGTGCTT
ChIP NC *Ccnd1* F	ChIP-qPCR	ATGCATGCACAGACACAGGT
ChIP NC *Ccnd1* R	ChIP-qPCR	CTGGCCCATCTGCAATAGAT
ChIP *ERG* 1 F	ChIP-qPCR	GGTGCACATCTGCAGAAAGA
ChIP *ERG* 1 R	ChIP-qPCR	TTCAGCCCTGATAACCCATC
ChIP *ERG* 2 F	ChIP-qPCR	CTGTGCCCAGATGGGTTATC
ChIP *ERG* 2 R	ChIP-qPCR	CCTCCTCTTAACGGCTGATG
ChIP NC *ERG* F	ChIP-qPCR	AGAACTCTGGGCATGCTTGT
ChIP NC *ERG* R	ChIP-qPCR	TGATGGTGTTCGTGAGCATT
ChIP *CCND1* 1 F	ChIP-qPCR	GACCCCTTAGGGAATTCTGG
ChIP *CCND1* 1 R	ChIP-qPCR	TCCTCCCCTCACCTCTCC
ChIP *CCND1* 2 F	ChIP-qPCR	GAGGGGAGGAGGCGAGAG
ChIP *CCND1* 2 R	ChIP-qPCR	TTTTCTAAGCCTTACGGTAAACG
ChIP NC CCND1 F	ChIP-qPCR	GACAGCACGAATCACAATGG
ChIP NC *CCND1* R	ChIP-qPCR	GGTGGTGGGAAGAATCAGAA

369

370

Supplemental Table 3. GSEA report for positively enriched pathways in GFPhigh L-GMPs (C2 chemical and genetic perturbations)

	Pathway	SIZE	NES	NOM p-val	FDR q-val	FWER p-val
1	KYNG_DNA_DAMAGE_BY_UV	51	2.81	0	0.168	0
2	BOSCO_INTERFERON_INDUCED_ANTIVIRAL_MODULE	62	2.57	0	0.168	0.168
3	BOYLAN_MULTIPLE_MYELOMA_PCA3_DN	61	2.53	0	0.168	0.168
4	KIM_WT1_TARGETS_UP	199	2.52	0	0.168	0.168
5	LUI_THYROID_CANCER_CLUSTER_1	46	2.52	0	0.168	0.168
6	ICHIBA_GRAFT_VERSUS_HOST_DISEASE_35D_UP	127	2.5	0	0.168	0.168
7	GAL_LEUKEMIC_STEM_CELL_DN	204	2.5	0	0.168	0.168
8	RICKMAN_TUMOR_DIFFERENTIATED_WELL_VS_POORLY_DN	334	2.45	0	0.168	0.168
9	ICHIBA_GRAFT_VERSUS_HOST_DISEASE_D7_UP	99	2.44	0	0.168	0.168
10	LEE_TARGETS_OF_PTCH1_AND_SUFU_UP	48	2.44	0	0.168	0.168
11	GROSS_HYPOXIA_VIA_HIF1A_DN	99	2.43	0	0.168	0.168
12	KYNG_DNA_DAMAGE_DN	162	2.41	0	0.168	0.168
13	LANDIS_ERBB2_BREAST_TUMORS_324_UP	141	2.4	0	0.168	0.168
14	MARTIN_VIRAL_GPCR_SIGNALING_UP	75	2.39	0	0.168	0.168
15	PROVENZANI_METASTASIS_DN	121	2.39	0	0.168	0.168
16	AMUNDSON_DNA_DAMAGE_RESPONSE_TP53	15	2.38	0	0.168	0.168
17	LEE_AGING_NEOCORTEX_DN	54	2.38	0	0.168	0.168
18	WOTTON_RUNX_TARGETS_UP	17	2.37	0	0.168	0.168
19	DELYS_THYROID_CANCER_UP	382	2.36	0	0.168	0.168
20	MAGRANGEAS_MULTIPLE_MYELOMA_IGLL_VS_IGLK_UP	38	2.35	0	0.168	0.168

Supplemental table 4. GSEA report for positively enriched pathways in GFPhigh L-GMPs (C5 Gene Ontology biological process)

	Pathway	SIZE	NES	NOM p-val	FDR q-val	FWER p-val
1	GOBP_POSITIVE_REGULATION_OF_NIK_NF_KAPPAB_SIGNALING	62	2.9	0	0.163	0
2	GOBP_GANGLIOSIDE_METABOLIC_PROCESS	22	2.84	0	0.163	0.163
3	GOBP_HEMATOPOIETIC_STEM_CELL_DIFFERENTIATION	26	2.84	0	0.163	0.163
4	GOBP_CELLULAR_RESPONSE_TO_CORTICOSTEROID_STIMULUS	48	2.84	0	0.163	0.163
5	GOBP_NEGATIVE_REGULATION_OF_PROTEIN_BINDING	83	2.8	0	0.163	0.163
6	GOBP_RESPONSE_TO_MOLECULE_OF_BACTERIAL_ORIGIN	279	2.79	0	0.163	0.163
7	GOBP_LYMPHOCYTE_MEDIATED_IMMUNITY	233	2.76	0	0.163	0.163
8	GOBP_POSITIVE_REGULATION_OF_BINDING	152	2.74	0	0.163	0.163
9	GOBP_CELLULAR_RESPONSE_TO_ALCOHOL	73	2.74	0	0.163	0.163
10	GOBP_CORONARY_VASCULATURE_DEVELOPMENT	40	2.73	0	0.163	0.163
11	GOBP_POSITIVE_REGULATION_OF_B_CELL_ACTIVATION	78	2.73	0	0.163	0.163
12	GOBP_ANTIGEN_PROCESSING_AND_PRESENTATION	74	2.72	0	0.163	0.163
13	GOBP_LIPOPROTEIN_LOCALIZATION	16	2.69	0	0.163	0.163
14	GOMF_CARBOXYPEPTIDASE_ACTIVITY	38	2.69	0	0.163	0.163
15	GOBP_POSITIVE_REGULATION_OF_DEFENSE_RESPONSE	232	2.69	0	0.163	0.163
16	GOBP_B_CELL_MEDIATED_IMMUNITY	126	2.68	0	0.163	0.163
17	GOBP_PEPTIDYL_CYSTEINE_MODIFICATION	45	2.68	0	0.163	0.163
18	GOBP_MEMBRANE_INVAGINATION	76	2.68	0	0.163	0.163
19	GOBP_POSITIVE_REGULATION_OF_DNA_BINDING	47	2.65	0	0.163	0.163
20	GOBP_GLYCOLIPID_BIOSYNTHETIC_PROCESS	65	2.65	0	0.163	0.163

Supplemental table 5. GSEA report for positively enriched pathways in sh*Luc*-EVI1-AML cells vs. sh*Erg* (C5 Gene Ontology biological process)

	Pathway	SIZE	NES	NOM p-val	FDR q-val	FWER p-val
1	GOMF_STRUCTURAL_CONSTITUENT_OF_RIBOSOME	126	2.02	0	0.026	0.029
2	GOBP_NUCLEOBASE_CONTAINING_SMALL_MOLECULE_INTERCONVERSION	26	1.96	0	0.044	0.097
3	GOCC_RIBOSOMAL_SUBUNIT	152	1.94	0	0.042	0.135
4	GOBP_METAPHASE_ANAPHASE_TRANSITION_OF_CELL_CYCLE	60	1.92	0	0.058	0.239
5	GOBP_RIBOSOMAL_LARGE_SUBUNIT_BIOGENESIS	59	1.92	0	0.049	0.252
6	GOCC_SNO_S_RNA_CONTAINING_RIBONUCLEOPROTEIN_COMPLEX	26	1.91	0	0.046	0.28
7	GOBP_RIBOSOME_BIOGENESIS	275	1.91	0	0.042	0.293
8	GOCC_RIBOSOME	186	1.9	0	0.042	0.33
9	GOBP_RIBONUCLEOPROTEIN_COMPLEX_BIOGENESIS	399	1.9	0	0.039	0.335
10	GOBP_DNA_DEPENDENT_DNA_REPLICATION	148	1.9	0	0.035	0.341
11	GOBP_NCRNA_PROCESSING	362	1.89	0	0.033	0.347
12	GOBP_DNA_REPLICATION	263	1.89	0	0.032	0.366
13	GOCC_LARGE_RIBOSOMAL_SUBUNIT	93	1.89	0	0.03	0.368
14	GOBP_RRNA_METABOLIC_PROCESS	220	1.89	0	0.028	0.376
15	GOCC_CONDENSED_CHROMOSOME_CENTROMERIC_REGION	111	1.88	0	0.033	0.432
16	GOBP_MITOCHONDRIAL_GENE_EXPRESSION	160	1.88	0	0.032	0.445
17	GOBP_NCRNA_METABOLIC_PROCESS	432	1.87	0	0.033	0.477
18	HP_BICORNUATE_UTERUS	42	1.87	0	0.033	0.49
19	GOBP_MITOCHONDRIAL_TRANSLATION	132	1.87	0	0.031	0.492
20	GOBP_MITOTIC_SISTER_CHROMATID_SEGREGATION	152	1.86	0	0.031	0.513

Supplemental table 6. GSEA report for positively enriched pathways in sh*Luc*-EVI1-AML cells vs. sh*Ccnd1* in vitro (C5 Gene Ontology biological process)

	Pathway	SIZE	NES	NOM p-val	FDR q-val	FWER p-val
1	GOBP_RESPONSE_TO_TYPE_I_INTERFERON	76	2.23	0	0.003	0.002
2	GOBP_RESPONSE_TO_INTERFERON_GAMMA	149	2.19	0	0.003	0.004
3	GOBP_POSITIVE_REGULATION_OF_MACROPHAGE_MIGRATION	23	2.12	0	0.007	0.015
4	GOBP_RESPONSE_TO_INTERFERON_BETA	27	2.09	0	0.01	0.03
5	GOBP_TYPE_I_INTERFERON_PRODUCTION	118	2.05	0	0.017	0.061
6	GOBP_POSITIVE_REGULATION_OF_TUMOR_NECROSIS_FACTOR_SUPERFAMILY_CYTOKINE_ PRODUCTION	74	2.05	0	0.016	0.07
7	GOBP_MEMBRANE_RAFT_ORGANIZATION	22	2.04	0	0.017	0.087
8	GOBP_DEFENSE_RESPONSE_TO_VIRUS	203	2.03	0	0.016	0.092
9	GOBP_LYTIC_VACUOLE_ORGANIZATION	67	2.02	0	0.017	0.109
10	GOBP_POSITIVE_REGULATION_OF_TYPE_I_INTERFERON_PRODUCTION	70	2.01	0	0.018	0.125
11	GOBP_POSITIVE_REGULATION_OF_INTERFERON_BETA_PRODUCTION	30	2.01	0	0.018	0.133
12	GOBP_LATE_ENDOSOME_TO_VACUOLE_TRANSPORT	22	2.01	0.003	0.017	0.138
13	GOBP_MICROGLIAL_CELL_ACTIVATION	44	2	0	0.016	0.146
14	GOBP_INTERLEUKIN_6_PRODUCTION	125	2	0	0.016	0.157
15	GOBP_RELAXATION_OF_CARDIAC_MUSCLE	16	1.99	0.003	0.017	0.176
16	GOBP_INTERFERON_BETA_PRODUCTION	46	1.98	0	0.019	0.208
17	GOBP_POSITIVE_REGULATION_OF_INTERLEUKIN_6_PRODUCTION	70	1.98	0	0.018	0.21
18	GOBP_RESPONSE_TO_INTERFERON_ALPHA	19	1.97	0.002	0.019	0.232
19	GOBP_RESPONSE_TO_VIRUS	287	1.95	0	0.026	0.311
20	GOBP_POSITIVE_REGULATION_OF_NEUROINFLAMMATORY_RESPONSE	15	1.95	0	0.025	0.313

References

1. Yoshimi A, Goyama S, Watanabe-Okochi N, et al. Evi1 represses PTEN expression and activates PI3K/AKT/mTOR via interactions with polycomb proteins. *Blood*. 2011;117(13):3617-3628.
2. Arai S, Yoshimi A, Shimabe M, et al. Evi-1 is a transcriptional target of mixed-lineage leukemia oncoproteins in hematopoietic stem cells. *Blood*. 2011;117(23):6304-6314.
3. Kagoya Y, Yoshimi A, Kataoka K, et al. Positive feedback between NF-κB and TNF-α promotes leukemia-initiating cell capacity. *The Journal of clinical investigation*. 2014;124(2):528-542.
4. Mizuno H, Koya J, Masamoto Y, Kagoya Y, Kurokawa M. Evi1 upregulates Fbp1 and supports progression of acute myeloid leukemia through pentose phosphate pathway activation. *Cancer Sci*. 2021;112(10):4112-4126.
5. Langmead B, Salzberg SL. Fast gapped-read alignment with Bowtie 2. *Nat Methods*. 2012;9(4):357-359.
6. Nakato R, Shirahige K. Sensitive and robust assessment of ChIP-seq read distribution using a strand-shift profile. *Bioinformatics*. 2018;34(14):2356-2363.
7. Nakato R, Sakata T. Methods for ChIP-seq analysis: A practical workflow and advanced applications. *Methods*. 2021;187:44-53.
8. Mootha VK, Lindgren CM, Eriksson K-F, et al. PGC-1α-responsive genes involved in oxidative phosphorylation are coordinately downregulated in human diabetes. *Nat Genet*. 2003;34(3):267-273.
9. Subramanian A, Tamayo P, Mootha VK, et al. Gene set enrichment analysis: A knowledge-based approach for interpreting genome-wide expression profiles. *Proceedings of the National Academy of Sciences*. 2005;102(43):15545-15550.
10. van Galen P, Hovestadt V, Wadsworth Ii MH, et al. Single-Cell RNA-Seq Reveals AML Hierarchies Relevant to Disease Progression and Immunity. *Cell*. 2019;176(6):1265-1281.e1224.
11. Valk PJ, Verhaak RG, Beijen MA, et al. Prognostically useful gene-expression profiles in acute myeloid leukemia. *N Engl J Med*. 2004;350(16):1617-1628.
12. Oki S, Ohta T, Shioi G, et al. ChIP-Atlas: a data-mining suite powered by full integration of public ChIP-seq data. *EMBO Rep*. 2018;19(12).
13. Mandoli A, Singh AA, Jansen PW, et al. CBFB-MYH11/RUNX1 together with a compendium of hematopoietic regulators, chromatin modifiers and basal transcription factors occupies self-renewal genes in inv(16) acute myeloid leukemia. *Leukemia*.

2014;28(4):770-778.
14. Martens JH, Mandoli A, Simmer F, et al. ERG and FLI1 binding sites demarcate targets for aberrant epigenetic regulation by AML1-ETO in acute myeloid leukemia. *Blood*. 2012;120(19):4038-4048.
15. Mandoli A, Singh AA, Prange KHM, et al. The Hematopoietic Transcription Factors RUNX1 and ERG Prevent AML1-ETO Oncogene Overexpression and Onset of the Apoptosis Program in t(8;21) AMLs. *Cell Rep*. 2016;17(8):2087-2100.
16. Schütte J, Wang H, Antoniou S, et al. An experimentally validated network of nine haematopoietic transcription factors reveals mechanisms of cell state stability. *Elife*. 2016;5:e11469.
17. Assi SA, Imperato MR, Coleman DJL, et al. Subtype-specific regulatory network rewiring in acute myeloid leukemia. *Nat Genet*. 2019;51(1):151-162.
18. Vierstra J, Lazar J, Sandstrom R, et al. Global reference mapping of human transcription factor footprints. *Nature*. 2020;583(7818):729-736.

Supplemental figure 1

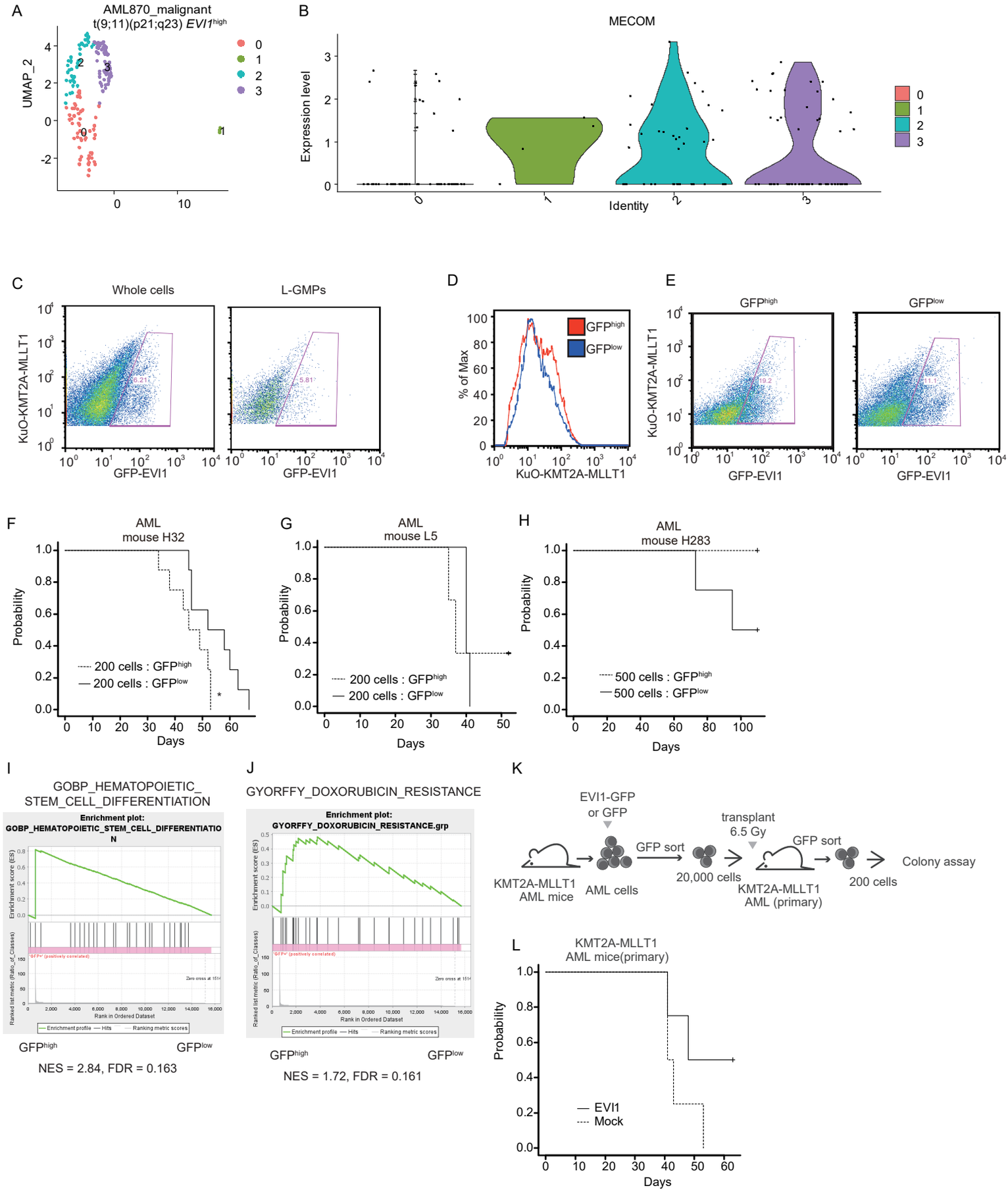

Supplemental figure 2

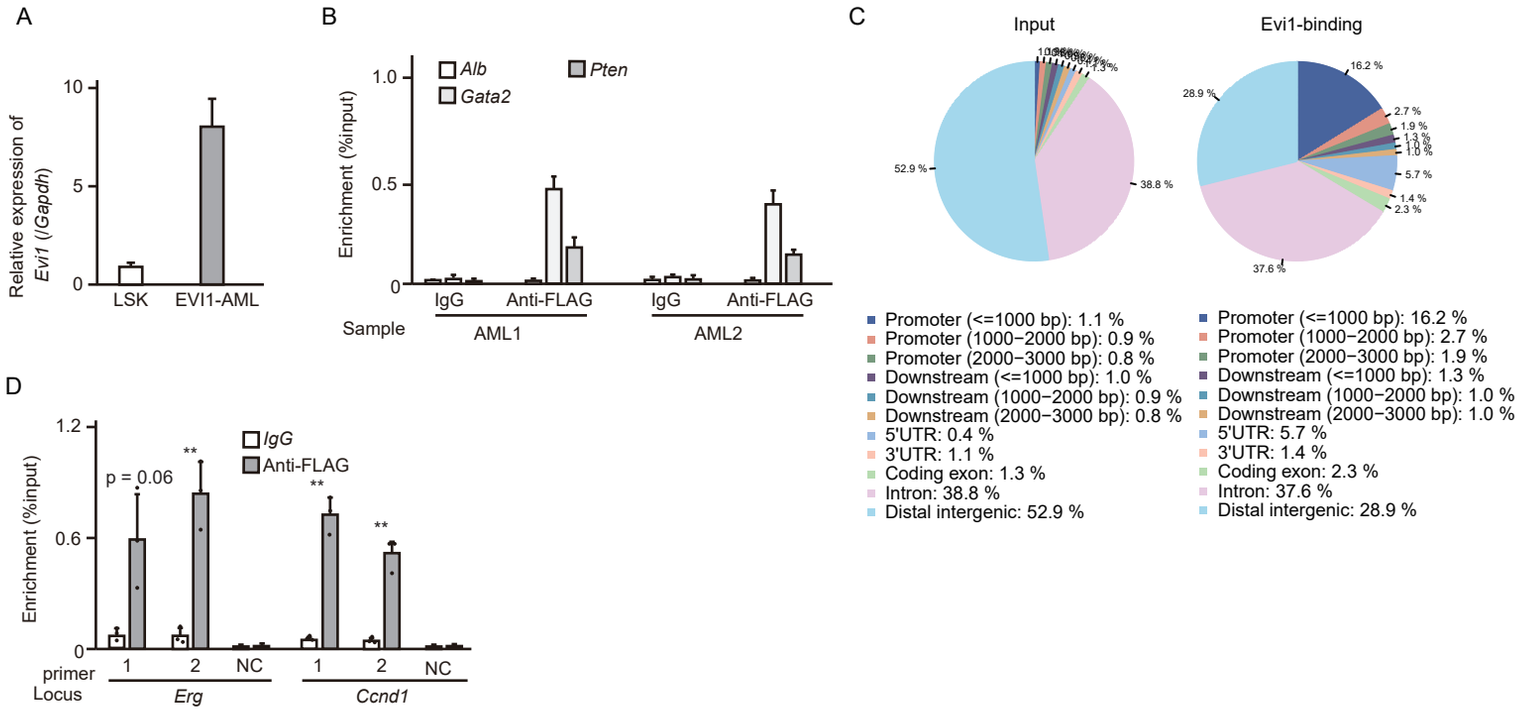

Supplemental figure 3

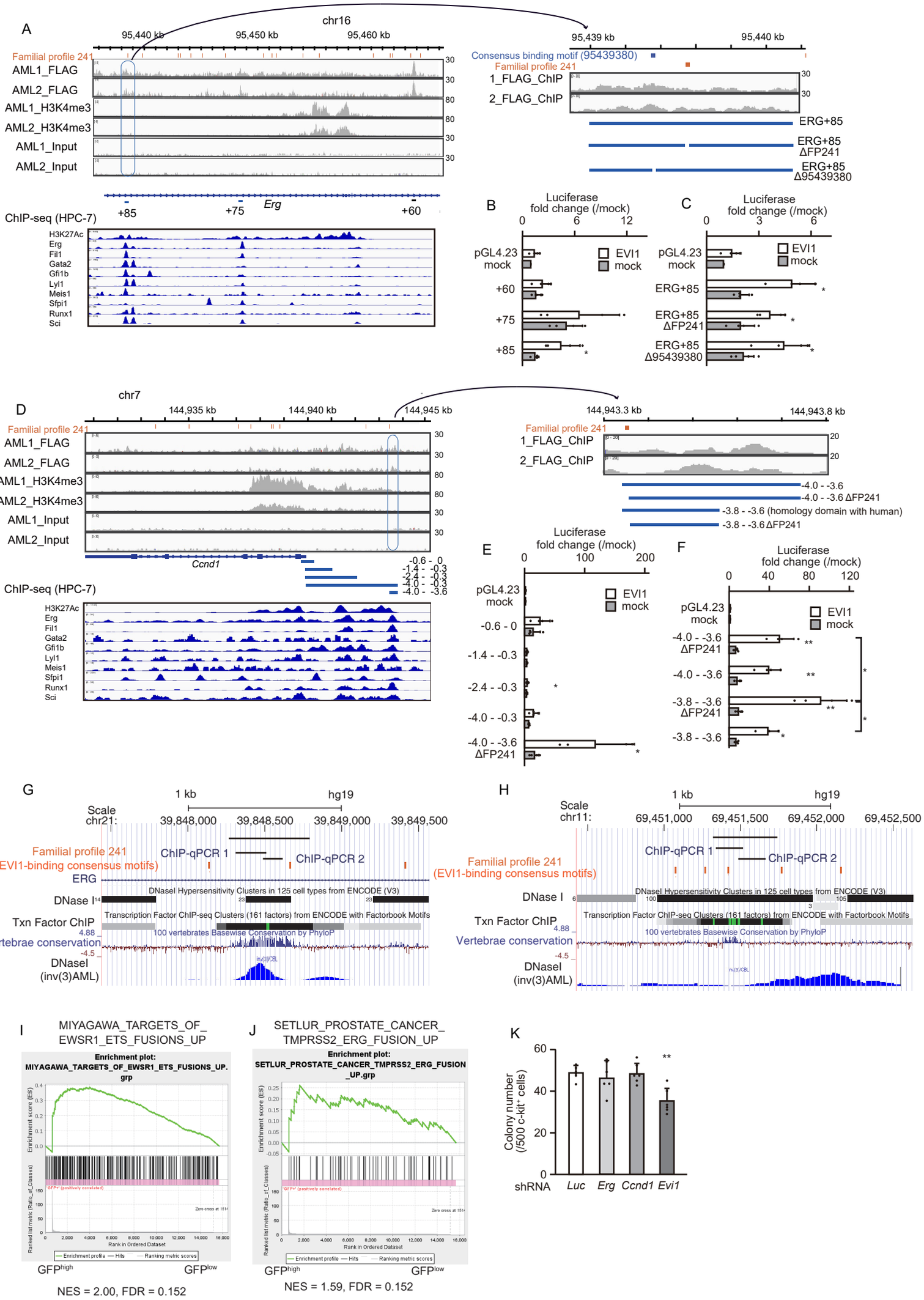

Supplemental figure 4

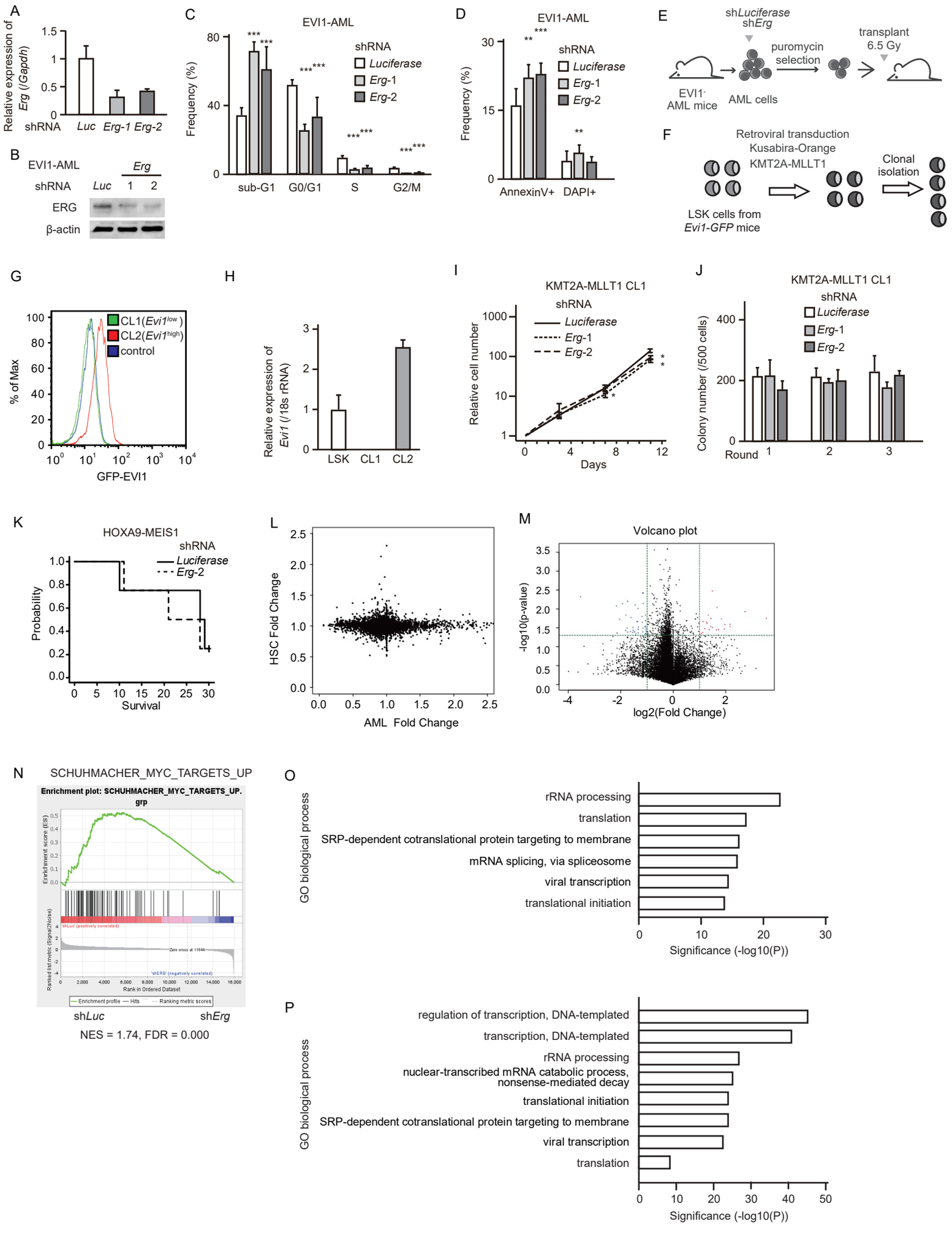

Supplemental figure 5

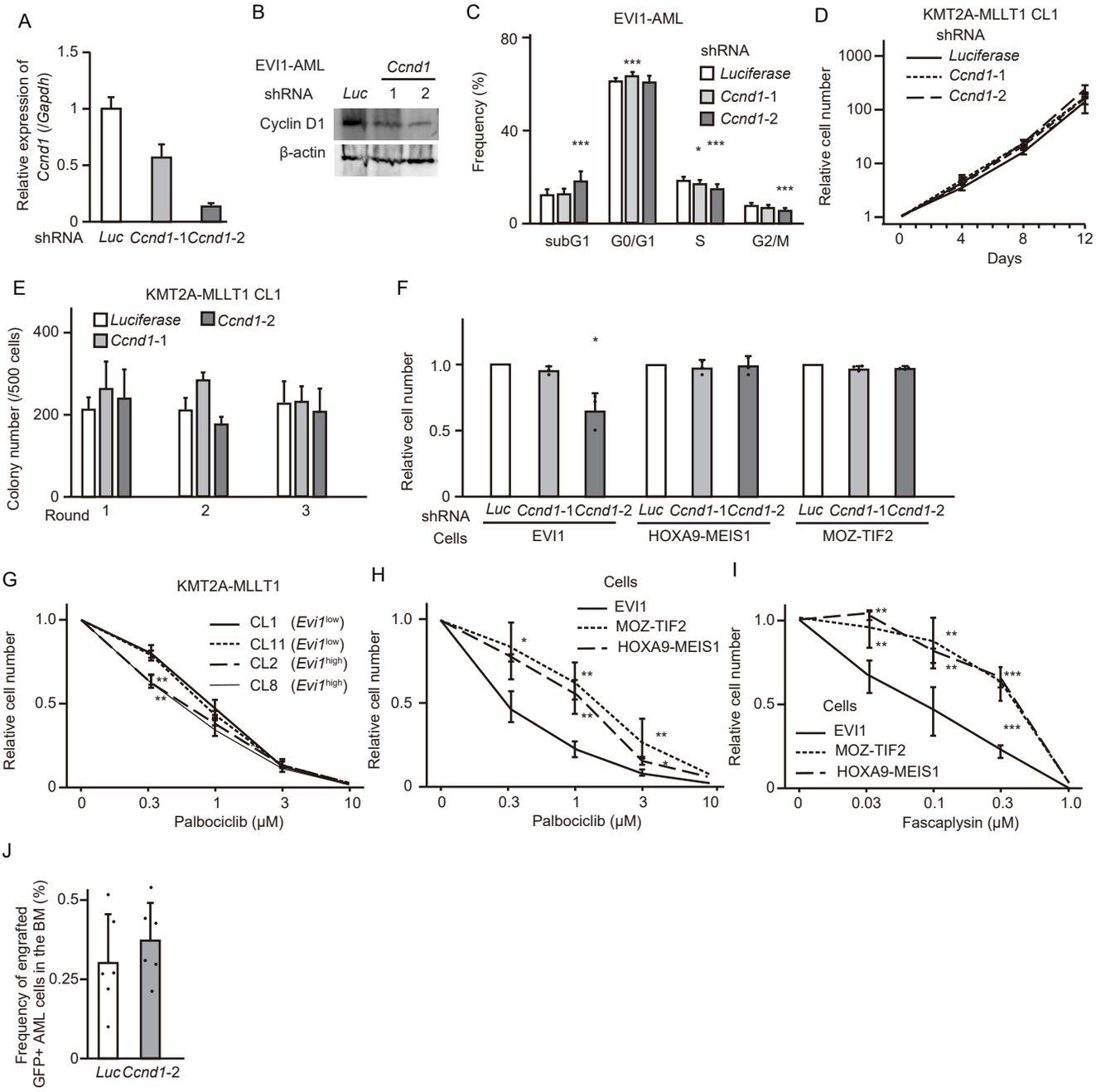

Supplemental figure 6

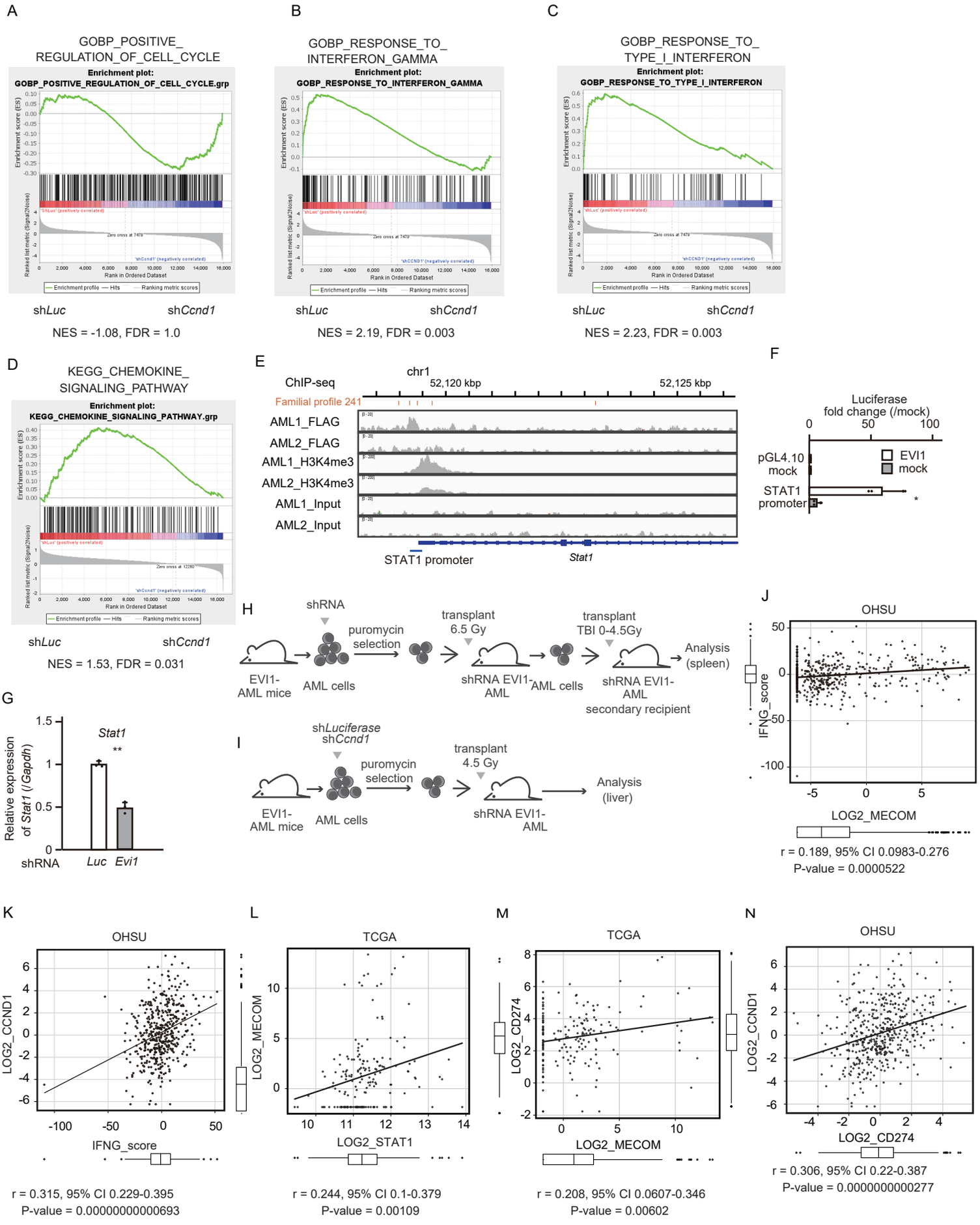

Supplemental figure 7